FOLIA HISTOCHEMICA ET CYTOBIOLOGICA
Vol. 45, No. 4, 2007
pp. 279-290

Review article

The ImageStream System: a key step to a new era in imaging

Ewa K. Zuba-Surma[1], Magdalena Kucia[1], Ahmed Abdel-Latif[3], James W. Lillard Jr.[2], and Mariusz Z. Ratajczak[1,4]

[1]Stem Cell Biology Program, University of Louisville, Louisville, KY, USA
[2]Brown Cancer Center, University of Louisville, Louisville, KY, USA
[3]Institute of Molecular Cardiology, University of Louisville, Louisville, KY, USA
[4]Department of Physiopathology, Pomeranian Medical University, Szczecin, Poland

Abstract: The aim of this article is to provide a brief review about the ImageStream system a novel tool for multiparameter cell analysis in flow. The instrument integrates the features of flow cytometry and fluorescence microscopy combined with a modern methodology for image analysis. Similar to flow cytometry, ImageStream allows analysis of a large number of cells based on their fluorescence features and provides statistical analysis of these features. Additionally, ImageStream allows detailed morphometric cellular analysis based on acquired cellular images integrating various morphometric and photometric features of the examined cells. Simply stated, ImageStream system is an advanced flow cytometer acquiring both integrated fluorescence signals as well as high quality fluorescence images and allowing muliparameter analysis. The innovative features of the instrument offer new analytical capabilities and allow for a multitude of possible applications beyond the current means of flow cytometry. While this article summarizes basic information about the features of ImageStream and its applications based on the available literature and it also describes our own experience.

Key words: ImageStream - Flow cytometry - Digital image analysis - Morphometry

Introduction

The history of imaging in the biological and medical sciences began in 1590 when Hans and Zachariah Janssen built the first microscope which then became functional in the 17th century after modifications introduced by Anton van Leeuwenhoek. Over the following decades, microscope technology has advanced by the development of more powerful and advanced optics that initiated a new era of basic and clinical cytology. Currently, the advanced features available in computerized microscopes have made them powerful tools for visualization and cellular analysis. This technology can be characterized by high spatial resolution and information content. However, the acquired images can not be simply converted into quantitative scores resulting in a high subjectivity of analysis. Another major limitation of microscopy is the low rate of image acquisition limiting its applicability for analysis of a large number of cells [1-4].

The next step in cellular analysis technology was the fruit of the combined effort of multi-disciplinary scientists and engineers, namely the flow cytometer, which measures light scatter and fluorescence intensity of cells in suspension and has significantly advanced the field. Andrew Moldavan introduced the idea of flow cytometry in 1934 but this prototype instrument was never built. In 1949, Wallace Coulter gave life to the flow cytometer when he built an instrument capable of counting blood cells in a fluidic stream. Based on Coulter's counter concept, Mack Fulwyler and Marvin Van Dilla at Los Alamos National Laboratory developed the first flow cytometric system which allowed the separation of particles according to their size [5-7]. This instrument was later advanced by adding fluorescence detection system and introduced by Leonard Herzenberg and his group at Stanford University as the first functional fluorescence-activated cell sorter (FACS) [7,8]. Concurrently, and independently of the Los Alamos and Stanford University group, Louis A. Kamentsky, who was initially affiliat-

Correspondence: E. Zuba-Surma, Stem Cell Biology Program, University of Louisville, 580 S. Preston St., Baxter II, Rm. 128, Louisville, KY 40202, USA; tel.: (+1502) 8523486, fax.: (+1502) 8523032, e-mail: ekzuba01@louisville.edu

ed with IBM (Watson Laboratory, NY), then with Bio/Physics, Inc (Mahopac, NY) and later with Ortho Instruments (Westwood Mass), constructed a flow cytometer consisting of flow chamber incorporated into UV light illuminated microscope; UV absorption and light scatter signal generated by the cells traversing the chamber were measured and computer recorded. This cytometer could measure up to 1,000 cells per second and was the first to analyze and record, in list mode fashion, several parameters attributed to a single cell. Designs of highly successful line of flow cytometers, initially offered by Bio/Physics and subsequently by Ortho Instuments (Cytograf, Cytofluorograf) incorporated many technical attributes developed by Kamentsky [9]. The evolution of flow cytometry continued in the 60s and 70s with a variety of modifications in both hardware and software.

The term "flow cytometry" was introduced in 1976 and is well known to scientists working in the fields of biology, medicine as well as other disciplines. Flow cytometry allows scientists to acquire a large number of events quickly. Data collected by flow cytometry allows statistical analysis of cellular populations as well as quantitative assessment of various features of acquired objects. This technique allows for the collection of data regarding the relative cellular size and granularity as well as fluorescence intensity signals creating opportunities for various applications [10-16].

However, the classic flow cytometer falls short of providing real images of the analyzed cells. Laser scanning cytometer (LSC) was the first technique that combined features of modern microscopy and the higher throughput features of flow cytometry [17-20]. LSC technology allows multiparametric analysis of individual cells on microscopic slides or multiwell plates and can analyze both photometric and morphometric features of cells, leading the way for multiple applications in the research and clinical fields [21-23]. Nevertheless, this technology is still limited by the number of cells analyzed and does not allow analysis of cells in suspension without first adhering them to a solid substrate which can introduce artifacts. Excellent review articles describing LSC microscopy as well as its various applications have been published by Darzynkiewicz and Kamentsky *et al.* [17-20].

The next milestone in the development of image technology and flow cytometry has been achieved with the introduction of the ImageStream (IS) cytometer. The IS combines the capabilities of a flow cytometer with the high resolution imaging of a fluorescent microscope. When compared with LSC, the IS provides the advantage of acquiring images of cells in suspension at a relatively high rate. The unique features of the IS are not confined only to image acquisition but also to the image analysis capabilities of the analytical program IDEAS which provides spectrophotometric and morphometric analysis tools. These features become important when analyzing cells undergoing morphological changes. The IS is capable of acquiring images from individual cells that have responded to various stimuli as well as the response of the whole population. The IDEAS analysis program allows quantitative measurements of size, shape, texture, and location of probes within, on or between cells. Because measurements are performed on individual cells, it is also possible to execute complex assays such as evaluating transcription factor translocation in rare subsets of cells, correlating apoptosis to the phase of cell cycle, distinguishing the cell type that has phagocytized particles, amongst a growing list of applications. In the current review we will examine the advance features of the IS technology as well as the research and potential clinical applications of this system.

ImageStream overview

The ImageStream system developed by Amnis Corporation is the first commercially available imaging flow cytometer with full integration of modern image analysis system (www.amnis.com). The innovative instrument combines the features of classic fluorescence microscopy and flow cytometry.

The main advantage of flow cytometry is its ability to analyze large number of cells in suspension collecting multicolor fluorescence intensity signals in a brief period of time. The introduction of multiple lasers, detectors, configurations of filters and beam splitters allows the detection of emitted fluorescence of various wavelengths through multiple channels. Advanced software and computers that perform compensation as well as statistical analysis and data display are the major part of a modern flow cytometric system.

Similar to flow cytometry, the ImageStream analyzes cells in suspension. Samples are introduced into a fluidic system where cells are hydrodynamically focused into a core stream and illuminated by a brightfield light source and a variable power 488 nm solid-state laser. Recently 405nm and 658nm lasers can be added and used interchangeably increasing the capacity of the system. Transmitted light, scattered light and emitted fluorescence are collected by a microscope objective and further fluorescence light is decomposed into six images in defined ranges of wavelengths by a dichroic filter stack. Signals are further directed onto the surface of a CCD camera with six channels employed as the detectors of the system [24] (Fig. 1). By this technique, the combined image is optically split into a set of six subimages including four fluorescence images (corresponding to 4 fluorescence signals collected in multicolor flow cytometry) as well as brightfield and darkfield images. Standard detectors (PMTs - photomultiplier tubes) commonly used in

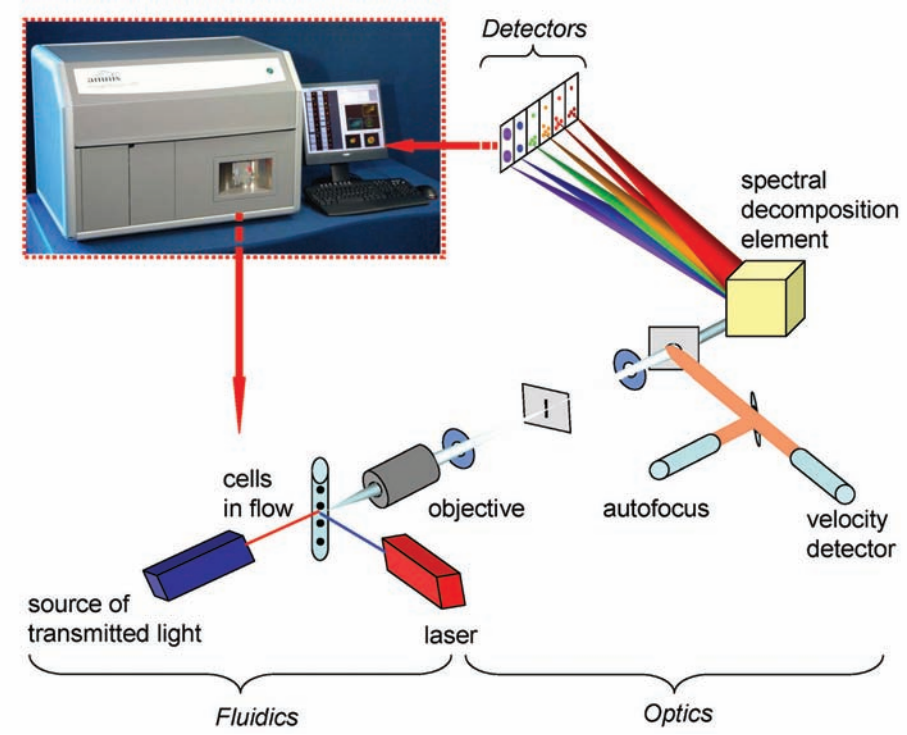

Fig 1. Image Stream platform overview. Cells in laminar flow were hydrodynamically focused into a glass cuvette and illuminated by laser (488nm) and red brightfield illumination light. Fluorescent, transmitted and scattered lights collected by objective were split into multi-spectral bands by optical decomposition element. Six independent wavelengths were collected by detectors - charge coupled device (CCD) camera (channels 1-6) and digital images were saved for further analysis by IDEAS software. (Adapted from Amnis Corp. materials; www.amnis.com).

flow cytometry have been replaced in the ImageStream system by a charge coupled device (CCD) camera (Fig. 1).

The process of spectral decomposition into six subimages and multispectral data collection allow: (i) simultaneous detection of brightfield, darkfield, and multiple fluorescence images (multimode imaging); (ii) separate quantification of signals from overlapping regions of the analyzed cell; (iii) calculation of both standard flow cytometric parameters as well as various morphologic features (e.g., cell area, perimeter, aspect ratio, texture, spot counts, cell centroid, gradient intensity, and spatial frequency) [24].

The optical features of the ImageStream system include a 0.75 numerical aperture lens objective and the 0.5 μm pixel size of the CCD in object space that allows high resolution imaging with event acquisition rates exceeding 100 cells per second. Hence, the CCD camera converts photons from the transmitted, scattered and emitted fluorescent light into photocharges in an array of pixels.

The high sensitivity of the instrument is achieved by operating the CCD camera in Time Delay Integration (TDI) mode. TDI imaging is a method of electronically panning the detector to track object motion. TDI detector mode increases signal collection time and preserves sensitivity and image quality even with fast relative movement between the detector and the objects (cells) [24,25]. The current ImageStream instrument collects images continuously acquiring a signal of 10 milliseconds duration per object on average as a result of TDI and resulting in about at approximately 3 megabytes per second of data accumulation. This allows the detection of low fluorescence intensity signals even when the cell image is acquired at high speed [24].

In post-acquisition image processing, the six channel images of each object are corrected into spatial registry and spectral overlap is compensated pixel by pixel using image collected from single fluorochrome stained cell populations without bright field illumination [26,27]. This is followed by the calculation of more than 200 various morphometric and photometric features for each cell. The analysis and display methods, together with the well-developed compensation feature allow co-localization of fluorescence and morphological signals in cells as well as measurement of signals from various fluorescent probes. The results are stored in a compensated image file (CIF) for analysis. Data files containing the information from 10.000-20.000 cells are about 200 MB in size and can be stored and analyzed using standard personal computers.

Advantages of ImageStream system over other imaging tools

The ImageStream possesses the ability for multi-spectral imaging of a large number of cells traveling in a flow stream by combining microscopy and flow cytometry in a single platform. The advantage of using this system in comparison to fluorescent microscopy is its ability to analyze imagery from a large number of cells acquired in suspension. This provides a unique

opportunity for statistical analysis of large populations, but also aids in avoiding artifacts. The analysis of collected data is also more quantitative with the ImageStream system when compared with conventional microscopy [28,29].

The information obtained based on image analysis can be fully integrated with the statistical analysis of cellular populations, a feature typical for flow cytometry.

Cellular subpopulations can be identified and quantified not only based on photometric parameters of cells, but also by the morphological features of the cells and their nuclei. Photometric and morphometric parameters based on collected cellular imagery can be compared, thus creating novel options for defining subpopulations and opening a new era in cellular analysis. These analytical methods are a common feature between the ImageStream technology and laser scanning cytometry (LSC). However, in contrast to LSC systems, the ImageStream acquires imagery from a large number of cells in suspension. This technology enables the examiner to evaluate unique morphological features of cells simultaneously with the acquisition and analysis of many objects in a short period of time [17,24].

The ImageStream can be useful in novel experimental applications when the location of signals in cells is as important as statistical analysis of fluorescence intensity data from cell populations. Images saved during acquisition can be used not only to measure various morphological characteristics of each cell, but also fluorescence intensity-based parameters used in standard flow cytometry. Similar to conventional flow cytometry, correct compensation of spectral crosstalk is essential for the quantification of image-based data. The guidelines for compensation are conceptually similar to those applied for flow cytometric data [30]. However, it involves some additional data processing steps, which are described in detail by Ortyn and colleagues [26]. Spectral compensation insures that all the light measured in any given channel comes from a single source. Once the data are compensated, many different fluorescence based measurements can be obtained from the collected images [26,31].

Over 200 intensity-based and morphological parameters are available to be analyzed for every cell. However, most of these parameters are not yet used in research/clinical applications. These parameters can be compared on dot-plots or visualized individually on histograms. Subpopulations of cells can be identified not only based on intensity of fluorescence, like in flow cytometry, but also according to morphometric features. Additionally, custom parameters can be further refined. The combination of spatial alignment and spectral compensation is unique to the ImageStream and allows quantitative measurements of probe localization. The applications include nuclear translocation of probes, co-localization of probes and estimation of distance between two probes. These applications are based on features such as Similarity, Similarity bright detail, and Radial Delta Centroid, respectively [31-33].

During analysis, single or multiple objects displayed on dot-plots and histograms can be directly visualized in image galleries. This useful option allows the user to verify the gating strategy and include the maximal number of objects in the analysis. Further, the ImageStream technology can localize and quantitatively determine fluorescence in defined subcellular compartments including cytoplasm, nucleus, endosomes, lysosomes and the cell surface membrane. It also allows co-localization of different fluorescent signals in the entire cell or within selected cellular compartments. This feature is used to determine the co-localization of various membrane receptors, organelle uptake of tagged proteins, and translocation of transcription factors from cytoplasm to nuclear region. The localization of fluorescent signals during cellular interactions such as the immune synapse formation also can be estimated by analysis of ImageStream data.

Applications

Various applications of Image Stream have been already described [24,28,29,31,32,34-37]. The examples below are selected from multiple possible applications. We have chosen to present these applications since they have been recently published in the scientific literature.

Apoptosis quantification

Since Kerr and colleagues described the biological phenomenon of apoptosis [38], various methods of apoptotic cell detection have been described. These methods include the analysis of cells in suspension or fixed and stained on solid carriers. Most of the detection assays are based on the cytochemical features characterizing apoptotic cells including morphology and composition of surface membrane, nuclear events and DNA fragmentation, cellular and nuclear dissolution, activation of cytoplasmic enzymes as well as functionality and integrity of mitochondria [39-47]. Detection of cell death can be further divided according to the methodology used. Morphological and structural changes of apoptotic cells can be detected by electrophoresis, ELISA, Western blotting, electron and fluorescence microscopy and fluorescence cytometry [40-52].

The ImageStream system can be of aid in the detection and quantification of apoptotic and necrotic cells by applying techniques for cell death detection origi-

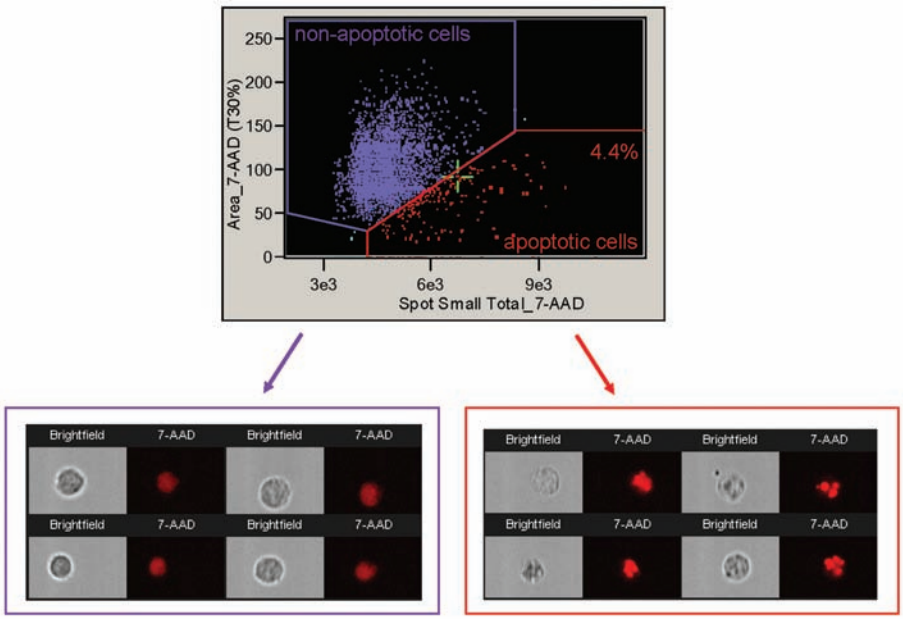

Fig. 2. Analysis of apoptosis based on nuclear fragmentation. Living and apoptotic Nalm-6 cells (human leukemia B cell line) were distinguished based on comparison of size and intensity of nuclear fluorescence, illustrating the process of DNA fragmentation. Living and apoptotic cells are enclosed in violet and red region of upper dot-plot, respectively. Cells were cultured in high density for 5 days and fixed with 2% paraformaldehyde and stained with 40 μM 7-AAD. Nuclei are presented as red and brightfield is shown as a transmission image. Apoptotic cells (right) with small, fragmented, highly textured nuclear images and were characterized by smaller area of nuclei and higher localized 7-AAD intensities compared to intact nuclei (left). 4.4% of cultured, untreated cells showed apoptotic features.

nally described for fluorescence microscopy and cytometry such as staining with nuclear dyes and Annexin V [24,35,47,50,51,53]. However, a significant limitation of this assay is the inability to distinguish between necrotic and late apoptotic cells. ImageStraem analyzes morphological parameters that can distinguish these two populations. Late apoptotic and necrotic cells have defective membrane integrity, which permits entry of 7-AAD giving false impression of larger nuclear area. However, necrotic cells produce less complicated and less heterogeneous side scatter images (darkfield) when compared to the apoptotic cells allowing distinguishing them during analysis. Comparison of image galleries from living, early and late apoptotic, and necrotic cells confirms the classification of each population [24].

The approach described above allows for a more detailed and precise analysis of the acquired images. Furthermore, the ImageStream permits a simple quantification of apoptosis based solely on the features of nuclei stained by DNA-intercalating fluorescent dyes. The chromatin of apoptotic cells condenses and fragments forming the characteristic spots of condensed heterochromatin inside nuclei. Apoptotic nuclei produce small, fragmented, highly textured nuclear images. This causes nuclear dyes to be localized to small punctate regions of the fragmenting nucleus. This feature can be detected by the analytical classifiers in IDEAS. The brightest 30% of the pixels in the apoptotic cell are in a small area of nuclei that can be identified by these analytical features. Because of the condensed chromatin, apoptotic cells have brighter fluorescence sequestered in small regions and thus higher quantitative scores with this classifier in IDEAS [24,35] (Fig. 2).

The ImageStream system is also capable of assessing apoptosis with techniques such as BRDU staining and nuclear fragmentations in a TUNEL assay [54] which is typically evaluated by either a fluorescent microscope or a standard flow cytometer [29,35,52,54-56]. Hall and colleagues used the ImageStream to evaluate cellular staining for apoptosis with the standard TUNEL technique. Based on cellular morphological features, they were able to discriminate true TUNEL positive apoptotic cells from normal cells with an attached TUNEL positive fragment. The discrimination was entirely based on visual analysis of cells and thus would not have been possible with a conventional flow cytometer. The authors also identified apoptotic cells on the basis of nuclear image morphology and were able to correlate TUNEL positive staining with nuclear fragmentation [29] (Fig. 3).

Analysis of features calculated by the ImageStream based on cellular and nuclear morphology as well as apoptotic markers such as TUNEL or Annexin V allows the true classification of live and apoptotic cells as well as the enumeration of the yield of true as well as false positives. The ability of the ImageStream to compare and combine morphometric and photometric measures of cells, which is not achievable with conventional flow cytometers, makes possible the classification of cellular populations in different stages of cell death. When combined with classical assays including secondary markers for apoptosis, the ImageStream can be used to illustrate the sequence of events as cells progress through apoptosis. By coordinating nuclear fragmentation with depolarization of the phosphatidylserine residues, caspase activation, and cellular blebbing, a more comprehensive picture of the apoptotic process can be studied.

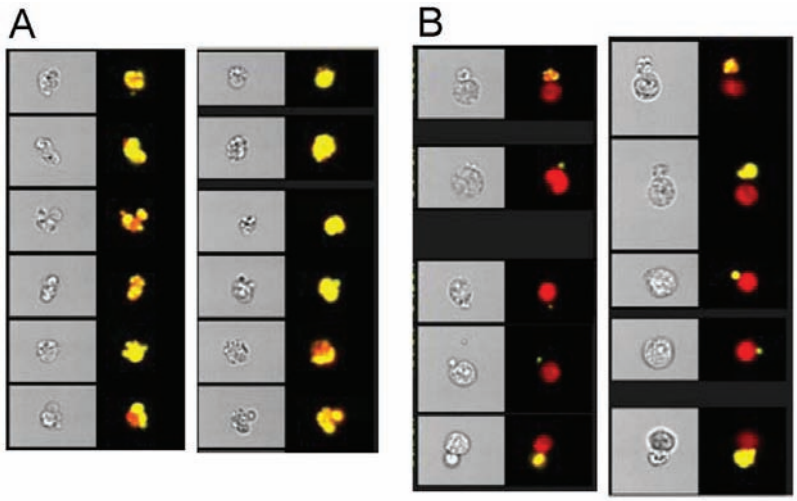

Fig. 3. Analysis of apoptosis using TUNEL technique. The TUNEL assay labels DNA strand breaks which are the hallmarks of apoptosis. Jurkat cells were treated with 1 μM CPT for 18 hrs to induce apoptosis and than fixed with 1% paraformaldehyde and 70% ethanol. Cells were stained with APO-BRDU TUNEL assay kit reagents (Phoenix flow Systems) and resuspended in a solution containing PI for further analysis by the IS. DNA breaks were identified as double positive cells labeled with anti-BRDU-FITC (green) and nuclei stained with PI (red). The figure highlights the ability to distinguish between true and false TUNEL-positive cells by examining image features. This capability cannot be achieved by standard flow cytometry. Apoptotic cells stained with PI and TUNEL show signal from broken DNA (FITC, green) and PI localized to the nucleus (red) (**A**). False positive cells can be identified on image galleries as intact cells with adherent DNA fragments attached to their surface (**B**). (Used with permission from Amnis Corp.).

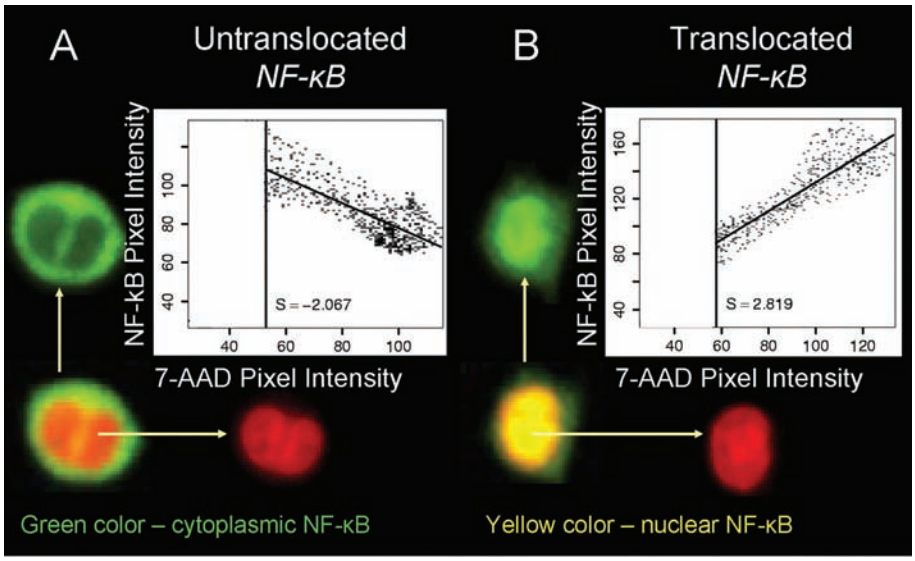

Fig. 4. Nuclear NF- B translocation - similarity feature. Representative images of THP-1 cells (human monocytic line) with untranslocated NF-κB residing in cytoplasm (**A**) and NF-κB translocated into the nuclear region (**B**). Cells were untreated or treated with 100 ng/ml LPS for 1 hour to induce NF-κB translocation. Cells were stained with FITC-anti- NF-κB and 7-AAD after fixation and permeabilization. Images show spectrally decomposed images of NF-κB (green), 7-AAD (red), and merged images of NF-κB and nuclei (7-AAD). Dot plots present correlations between NF-κB pixel intensity and intensity of nuclei (green and red fluorescence) as well as similarity score values for cells with and without NF-κB translocation. (Used with permission from Amnis Corp.).

Protein translocation analysis

Translocation of transcription factors (TFs) from cytoplasm to nucleus is part of the signaling pathways directly involved in gene expression initiated by extra- and intracellular stimuli and plays a pivotal role in cellular activation, differentiation and interaction. Activation and translocation of signal transduction proteins can be assessed by various techniques including flow cytometric and microscopic analysis based on fluorescence staining as well as a multitude of biochemical assays analyzing protein content of different cellular compartments [20,57-59]. LSC, an advanced imaging technology, with its ability to analyze large number of

cells seems to be an effective method for tracking the journey of translocated proteins from the cytoplasm to the nucleus in adherent cells [20,59].

The ImageStream, on the other hand, has the advantage of analyzing cells in suspension [31,35]. Using the ImageStream system, protein translocation can be measured by cross-correlation analysis of single fluorescence channel images obtained from cells with nuclei and transcription factors stained in separate colors. This approach was applied to measure protein translocation in cells with small cytoplasmic areas in a dose- and time-dependent manner, as well as in individual cell subsets contained in a mixed cell population [33]. Various methods for translocation tracking and quantification such as the similarity method and the nuclear to cytoplasmic intensity ratio method are applicable to fixed and stained cells and are performed on slides [17,20,59]. Further analysis techniques applied using the ImageStream system are optimal for estimating nuclear translocations in cells in suspension and more importantly in cells with a low nuclear-to-cytoplasm ratio [33,60].

George and colleagues [33] analyzed Nuclear Factor-kappa B (NF-κB) translocation in THP-1 cells after treatment with lipopolysacharide (LPS) using the ImageStream technology. Two populations of cells (with and without translocated NF-κB) were readily distinguishable using the cross-correlation analysis of nuclear NF-κB images from each cell instead of analysis of cytoplasm and nuclear area intensity ratios [33] (Fig. 4). The authors have measured nuclear translocation based on degree of colocalization of the NF-κB and nuclear fluorescence. For NF-κB nuclear translocation analysis, the data sources are the nuclear and NF-κB fluorescence images of the same cell. The data pairs are the pixel intensities at the same region in each image. The similarity score is derived from the Pearson's correlation coefficient, which is based on a regression analysis of pairs of intensity values taken from NF-κB and nuclear fluorescence images from single cellular images. For instance, if the images showed the NF-κB fluorescence signal surrounding and exclusive to a nuclear image, then the feature would show a negative correlation of pixel intensities between the two channels and subsequently a low score. If the pixel intensities of the NF-κB image coincided with the pixel intensities of the nuclear fluorescence image, then a positive correlation exists and a positive value would be generated. Comparing the pixel intensities of the nuclear and the transcription factor images on the same plot, an inverse or positive correlation indicates untranslocated or translocated cells, respectively. The slope of the linear regression line indicates the sign of the coefficient, while its magnitude reflects the degree by which the data fits to the regression line [33].

Similarity score and cross-correlation analysis methods can be also used to estimate the translocation of other transcription factors such as Interferon Regulatory Factor 7 (IRF-7), Forkhead-box (FOX) p3 (Foxp3) and p65 [31,33,34,60]. Percentage of cells with translocated transcription factors can be displayed on a histogram as cells with a high similarity score. The translocation event can be further confirmed using image galleries and visualizing cells with high similarity scores [33,34,60].

Co-localization and trafficking of proteins in various cellular compartments.

Acquiring information regarding the co-localization of specific soluble proteins and/or receptors in different cellular compartments can be critical for the understanding various biological processes and molecular interactions. Molecular co-localization or co-association of proteins can be determined using methods such as co-precipitation and yeast two-hybrid analysis as well as multiple fluorescent microscopy techniques [61-,65]. Moreover, the use of fluorescence labeled antibodies has been useful to estimate co-localization of surface membrane receptors (co-capping) [66,67].

Images acquired by the IS can be quantitatively analyzed for protein co-localization using the Similarity Bright Detail Score (SBDS). The SBDS quantifies the degree of similarity between any two channel images on a pixel by-pixel and cell-by-cell basis. The three-step process of SBDS calculation was recently described in details by Beum and colleagues [32]. This analysis allows co-localization of proteins with a resolution of 0.5 μm per pixel in the X and Y axis [32].

The ImageStream technology has also been used to demonstrate the mechanism of action of Rituxan (RTX), a widely used oncology therapeutic monoclonal antibody against CD20 molecule, by quantfying protein co-localization and trafficking using the SBDS algorithm [32]. The role of complement activation mediated by RTX was assessed based on the co-localization of Rituxan with C3b complement fragments. Both molecules were identified through specific fluorescent staining with antibodies conjugated to different fluorochromes. After image acquisition, the data was analyzed by an algorithm that measures the correlation of the RTX and C3b images on a pixel by pixel basis. Quantitative assessment of the degree of similarity between RTX and C3b fluorescent imagery was performed using a non-mean normalized version of Pearson's correlation coefficient and produced a value of Similarity Bright Detail Score (SBDS) for the double positive Rituxan/C3b cells [32,35] (Fig. 5).

The SBDS feature has also been applied to investigate the trafficking of proteins into different cellular

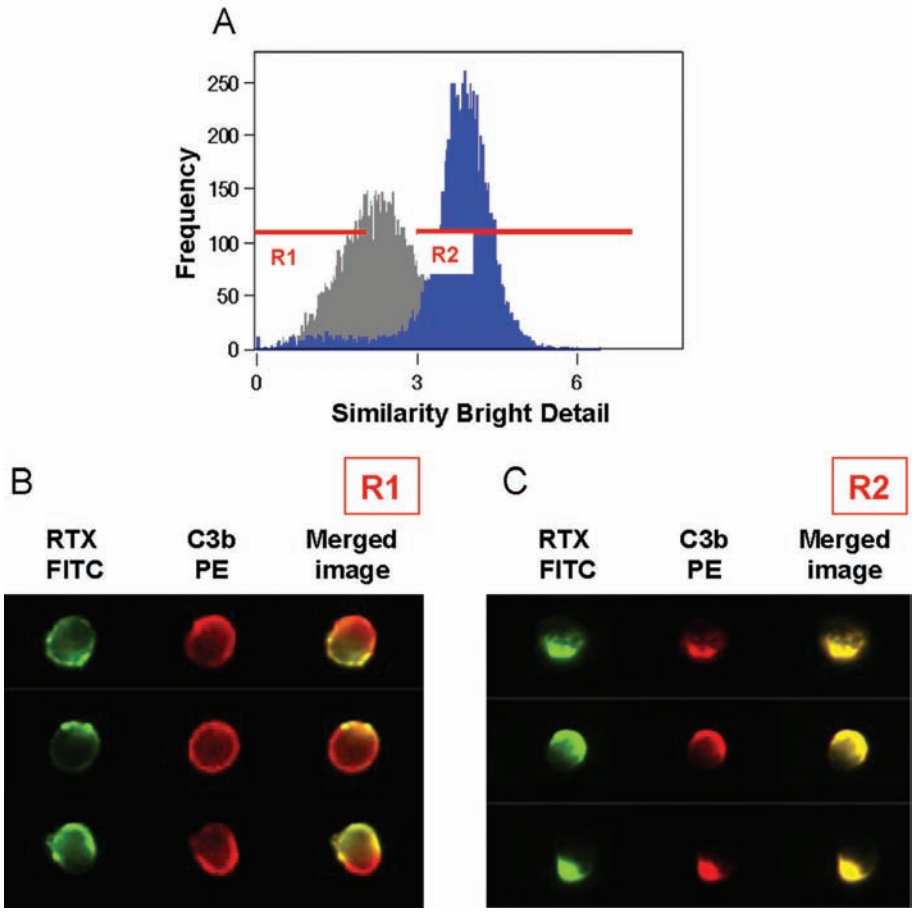

Fig. 5. Analysis of receptors co-localization. Co-localization of receptor binding C3b complement with receptor for Rituxan (RTX; anti-CD20 monoclonal antibody) may potentially indicate the role of RTX in complement-mediated killing. Raji cells (human B cell lymphoma line) were incubated with serum-derived complement components and RTX conjugated to FITC (green). Cells were additionally stained with PE-conjugated anti-C3b antibody (red). Histogram of Similarity Bright Detail (SBD) score between RTX and C3b images indicates that the majority of analyzed cells exhibited co-localization of RTX and C3b. Region R1 includes objects showing low co-localization, while region R2 encloses objects with co-localized C3b and RTX (**A**). The image gallery of objects enclosed in region R1 (**B**), while panel (**C**) illustrates cells with co-localized receptors visualized from region R2 (cells with high SBD score). (Used with permission from Amnis Corp.).

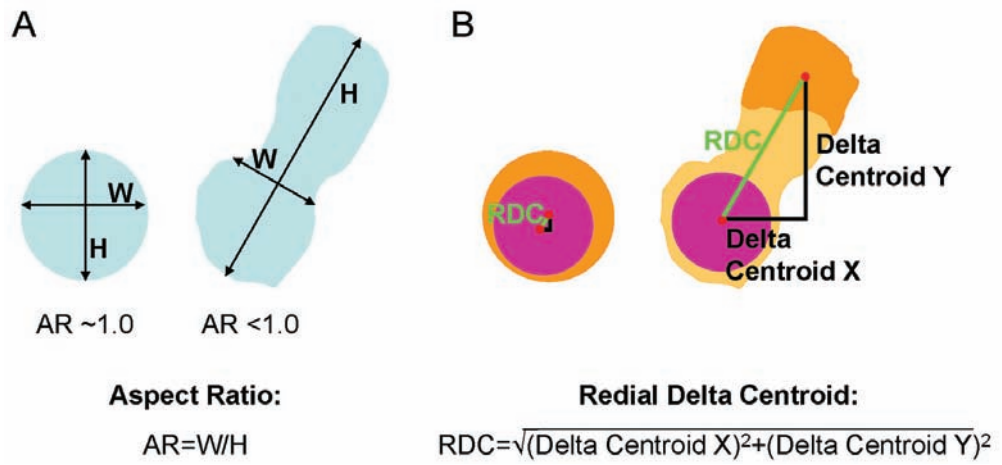

Fig. 6. Aspect ratio (AR) and Radial Delta Centroid (RDC) calculation. Formulas for the Aspect Ratio (**A**) and Radial Delta Centroid (**B**) calculations are presented schematically. **A**. Differences in aspect ratio value in relation to the shape of cells. Round, nonelongated cells have aspect ratio values close to 1.0, while the aspect ratio of cells forming pseudopods is much lower. Aspect ratio is calculated based on the brightfield image as the ratio of cellular minor axis (width; W) to major axis (height; H). **B**. The formula of radial delta centroid and its relation to the shape of cell. Radial delta centroid is measured as the distance from the center of the nuclear image to the center of the image of protein(s) involved in pseudopod formation (red dots) using the Pythagorean Theorem (green lines). If the protein is uniformly distributed throughout the cellular membrane (orange) and around the nucleus (violet), the radial delta centroid value is small when the nucleus is centered in the cytoplasm and larger when the protein is capped to one side of the membrane. The difference is related to the distance between the geometrical centers of staining for the images in the 2 respective channels. (Adapted from Amnis Corp. materials; www.amnis.com).

Table 1. List of fluorochromes and fluorescent probes compatible with the ImageStream system (all dyes are excited by 488nm laser)

Channel 3 (500-560nm)	Channel 4 (560-595nm)	Channel 5 (595-660nm)	Channel 6 (660-735nm)
FITC	PE	7-AAD	DRAQ-5
Alexa Fluor 488	Cy3	Propidium Iodide	PE-Cy5
Spectrum Green	DSRed	PE-Texas Red	PE-Cy5.5
eGFP	Alexa Fluor 555	R-PE-Alexa Fluor 610	R-PE-Alexa Fluor 680
eYFP	PKH26	QD-655	R-PE-Alexa Fluor 647
SYTO 16			PerCP
YOYO-1			PerCP-Cy5.5 (TruRed)
YOPRO-1			QD-705
MitoTracker green			
SYTOX Green			
Fluo-3			

Table 2. ImageStream system features - summary

Image Stream features	
Hardware ability	Uses CCD cameras working in TDI mode to collect images which allows analysis of cells in flow
	Collects 6 independent images of the cell in 6 separate channels
	Acquires images of 300 cells/second
	Allows to employ the most common fluorescent dyes excited by 488nm laser
	Generate images with 0.5 pixel resolution
Software ability	Allows quantitative analysis of individual cells and cellular populations at the same time in the same experiment
	Quantifies >200 morphometric and photometric features per cell
	Employs dot-plots and histograms for visualization of analyzed features allowing statistical calculations
	Allows identification of single object (dot) on plot or gated population based on their imaginary
	Requires usage of compensation matrix for color separation during analysis

compartments. Using fluorescent staining specific for endosomal and lysosomal compartments (early endosomal antigen 1 and Lamp1 antigens, respectively), it was possible to estimate intracellular localization of RTX uptake by cells by ImageStream data acquisition and analysis [35].

Shape Change Assay

Recently, the ImageStream technology was recently applied to the assessment of cellular shape change. The ImageStream system can be used to quantify cells during or after the process of changing their shape or pseudopod formation [37]. This system can distinguish between rounded and elongated cells based on calculation of Aspect Ratio value (AR). The AR value in the brightfield image is defined as the ratio of minor axis (width) to major axis (height) and is 1.0 for circular objects, while elongated cells have values significantly less than one (Fig. 6A).

Analytical approaches in IDEAS also distinguishes cells forming pseudopods from others based on polarization of proteins involved in this process such as Podocalyxin (Podo) distribution on the elongated side of membrane [37]. The feature can be calculated using the Radial Delta Centroid (RDC) function. RDC is estimated by measuring the radial distance between the geometrical centers of the nuclear image and the fluorescent image of the podocalyxin stain. The RDC is then calculated using the Pythagorean theorem (Fig. 6B). DNA is stained with 1,5-Dihydroxyanthraquinone (DRAQ5; fluorescent DNA binding dye) and Podo with fluorochrome conjugated antibodies [37].

If the Podo protein is uniformly distributed throughout the membrane and is visible around the nucleus, the RDC value is smaller than the case when the Podo protein is capped to one side of the membrane. Plotting the RDC between the nuclear and Podo image distribution together with the aspect ratio of the brightfield image allows identification of three cellular populations: i) capped cells (migration of podo staining to one pole of the cell), ii) pseudopod forming cells (elongated) and iii) rounded population (nonelongated with Podo uniformly distributed in membrane) [37]. Using these classifiers the percentage of each population can be quantified and the three populations can be confirmed by representative image galleries [37].

The multitude of features calculated by the ImageStream system provides a wide range of applications for cellular phenotyping and characterization. Combining the photometric features of four independent fluorescent signals with various morphological parameters creates future prospects for using ImageStream technology.

Other applications

The ImageStream system has also been used for: i) cell classification and identification [28,36]; ii) identification of Fluorescence In Situ Hybridization (FISH) positive cells [35]; iii) identification of mitotically active cells characterized by expression of various specific markers [68,69]; iv) identification of immune synapses between T cells and antigen presenting cells (APC) [69].

Preparation of samples for Image Stream analysis

The ImageStream system has been designed for image analysis of a large number of cells in suspension. In general, samples for the ImageStream analysis should be prepared in a fashion similar to standard flow cytometry methodologies [70]. Freshly isolated as well as fixed cells can be analyzed. For fixation purposes 2-4% of paraformaldehyde solution or commercially available fixation buffers have been used [24,26,28,32,34]. Surface antigen staining is recommended before fixation and can be performed according to standard flow cytometric procedures [70].

When staining for intracellular proteins, a permeabilization step is necessary. Widely accepted permeabilization agents include TritonX-100, saponin or methanol [26,28,32]. Fluorochromes selected for analysis need to be excitable by the 488 nm laser although a 405 nm laser and a 658 nm laser are available as upgrade options. Four independent fluorescent dyes can be chosen and matched to four ImageStream channels (Tab. 1). DNA binding dyes compatible with ImageStream imaging and analysis include propidium iodide (PI), 7-aminoactinomycin (7-AAD) and dihydroxyanthraquinone (DRAQ5) and they can be used for staining according to vendors' protocols [24,26,28,31,35,36,68]. Both 7-AAD and PI are viable cell impermeant dyes and thus can be used to determine cellular viability. If all of the cells need to be stained by 7-AAD or PI, a fixation step is required before staining [53,71,72]. DRAQ5 effectively intercalate into DNA of living as well as fixed cells [73-75]. Experimental design should include also single color stained control samples which are necessary for calculating the compensation matrix. Stained cells should be washed and resuspended in 50-100 l of PBS or other media in optimal concentration of 2-4x107/ml [26,33].

Summary and future perspectives

The ImageStream system has been developed as the next stage of modern flow cytometry, further expanding its analytical capabilities. Based on combined analysis of photometric as well as morphometric features of cells, the system can be uniquely applied to a multitude of research and clinical applications (Tab. 2). The ImageStream technology allows scientists the unique opportunity to combine statistical analysis of large number of cells while discerning multicolor images through combining the features of modern flow cytometry and fluorescence microscopy in one system. The ImageStream has become a powerful tool for image analysis. In the future, when additional lasers and optical parts are available, it will bring new possibilities for using various combinations of dyes and fluorescent probes. Based on this we can already imagine and plan new applications for this system in our research.

Acknowledgments: We would like to thank Philip J. Morrissey and Brian E. Hall (Amnis Corporation) for their critical revision of manuscript and providing the figures.

References

[1] Johnson LG. Applications of imaging techniques to studies of epithelial tight junctions. *Adv Drug Deliv Rev.* 2005;57: 111-121.
[2] Torchilin VP. Fluorescence microscopy to follow the targeting of liposomes and micelles to cells and their intracellular fate. *Adv Drug Deliv Rev.* 2005;57:95-109.
[3] Egner A, Hell SW. Fluorescence microscopy with superresolved optical sections. *Trends Cell Biol.* 2005;15:207-215.
[4] Jones CW, Smolinski D, Keogh A, Kirk TB, Zheng MH. Confocal laser scanning microscopy in orthopaedic research. *Prog Histochem Cytochem*. 2005;40:1-71.
[5] Fulwyler MJ. Electronic separation of biological cells by volume. *Science*. 1965;150:910-911.
[6] Robinson JP. Mack Fulwyler in his own words. *Cytometry Part A*. 2005;67A:61-67.
[7] Herzenberg LA. FACS innovation: a view from Stanford. *Clin Invest Med*. 2004;27:240-252.
[8] Hulett HR, Bonner WA, Barrett J, Herzenberg LA. Cell sorting: automated separation of mammalian cells as a function of intracellular fluorescence. *Science*. 1969;166:747-749.
[9] Kamentsky LA, Melamed MR, Derman H. Spectrophotometer: new instrument for ultrarapid cell analysis. *Science*. 1965; 150:630-631.
[10] Shapiro HM. Multistation multiparameter flow cytometry: a critical review and rationale. *Cytometry*. 1983;3:227-243.
[11] Radcliff G, Jaroszeski MJ. Basics of flow cytometry. *Methods Mol Biol*. 1998;91:1-24.
[12] Jaroszeski MJ, Radcliff G. Fundamentals of flow cytometry. *Mol Biotechnol*. 1999;11:37-53.
[13] Maftah A, Huet O, Gallet PF, Ratinaud MH. Flow cytometry's contribution to the measurement of cell functions. *Biol Cell*. 1993;78:85-93.
[14] Stewart CC. Clinical applications of flow cytometry. Immunologic methods for measuring cell membrane and cytoplasmic antigens. *Cancer*. 1992;69:1543-1552.
[15] Davey HM. Flow cytometric techniques for the detection of microorganisms. *Methods Cell Sci*. 2002;24:91-7.
[16] Arora SK. Analysis of intracellular cytokines using flowcytometry. *Methods Cell Sci*. 2002;24:37-40.
[17] Darzynkiewicz Z, Bedner E, Li X, Gorczyca W, Melamed MR. Laser-Scanning Cytometry: A New Instrumentation with Many Applications. *Exp Cell Res*. 1999;249:1-12.

[18] Kamentsky LA, Burger DE, Gershman RJ, Kamentsky LD, Luther E. Slide-based laser scanning cytometry. *Acta Cytol*. 1997;41:123-143.
[19] Kamentsky LA. Laser scanning cytometry. *Methods Cell Biol*. 2001;63:51-87.
[20] Deptala A, Bedner E, Darzynkiewicz Z. Unique analytical capabilities of laser scanning cytometry (LSC) that complement flow cytometry. *Folia Histochem Cytobiol*. 2001;39: 87-89.
[21] Kamentsky LA, Kamentsky LD. Microscope-based multiparameter laser scanning cytometer yielding data comparable to flow cytometry data. *Cytometry*. 1991;12:381-387.
[22] Bowen WP, Wylie PG. Application of laser-scanning fluorescence microplate cytometry in high content screening. *Assay Drug Dev Technol*. 2006;4:209-221.
[23] Tarnok A, Gerstner AO. Clinical applications of laser scanning cytometry. *Cytometry*. 2002;50:133-143.
[24] George TC, Basiji DA, Hall B, et al. Distinguishing modes of cell death using the ImageStream multispectral imaging flow cytometer. *Cytometry A*. 2004;59A:237-245.
[25] Spibey CA, Jackson P, Herick K. A unique charge-coupled device/xenon arc lamp based imaging system for the accurate detection and quantitation of multicolour fluorescence. *Electrophoresis*. 2001;22:829-836.
[26] Ortyn WE, Hall BE, George TC, et al. Sensitivity Measurement and compensation in spectral imaging. *Cytometry A*. 2006;69A:852-862.
[27] Ortyn WE, Perry DJ, Venkatachalam V, et al. Extended depth of field imaging for high speed cell analysis. *Cytometry A*. 2007;71:215-231.
[28] Parsons CH, Adang LA, Overdevest J, et al. KSHV targets multiple leukocyte lineages during long-term productive infection in NOD/SCID mice. *J Clin Invest*. 2006;116:1963-1973.
[29] Hall B, George T, Basiji D, et al. Automated classification of apoptosis and artifact rejection of TUNEL positive cells. ISAC XXIII. Quebec, Canada; 2006.
[30] Roederer M. Spectral compensation for flow cytometry: Visualization artifacts, limitations, and caveats. *Cytometry A*. 2001;45:194-205.
[31] George T, Hall B, Zimmerman C, et al. Quantitation of nuclear translocation events using ImageStream multispectral imaging cytometry. *Cytometry A*. 2006;59A:121.
[32] Beum PV, Lindorfer MA, Hall BE, et al. Quantitative analysis of protein co-localization on B cells opsonized with rituximab and complement using the ImageStream multispectral imaging flow cytometer. *J Immunol Methods*. 2006;317:90-99.
[33] George TC, Fanning SL, Fitzgeral-Bocarsly P, et al. Quantitative measurement of nuclear translocation events using similarity analysis of multispectral cellular images obtained in flow. *J Immunol Methods*. 2006;311:117-29.
[34] Arechiga AF, Bell BD, Solomon JC, et al. Cutting edge: FADD is not required for antigen receptor-mediated NF-kappaB activation. *J Immunol*. 2005;175:7800-7804.
[35] Brawley J, George T, Hall B, et al. Fluorescent In Situ Hybridization In Suspension Analysis Using ImageStream Multispectral Imaging Flow Cytometry. *Cytometry A*. 2004; 59A:130.
[36] Morrissey P, George T, Hall B, et al. Cell classification in human peripheral blood using the Amnis ImageStream flow imaging system. *FASEB*. 2004;19:A920.
[37] Tan PC, McNagny KM, Hall B. Quantitative analysis of pseudopod formation with the ImageStream cell imaging system. Amnis Corp. Website. 2006. Available at: http://www.amnis.com/docs/notes/Quantitative-Pseudopod Formation.pdf, Accessed November 22, 2006.
[38] Kerr JF, Wyllie AH, Currie AR. Apoptosis: a basic biological phenomenon with wide-ranging implications in tissue kinetics. *Br J Cancer*. 1972;26:239-257.
[39] Sgonc R, Wick G. Methods for the detection of apoptosis. *Int Arch Allergy Immunol*. 1994;105:327-332.
[40] Willingham MC. Cytochemical methods for the detection of apoptosis. *J Histochem Cytochem*. 1999;47:1101-1110.
[41] Yasuhara S, Zhu Y, Matsui T, et al. Comparison of comet assay, electron microscopy, and flow cytometry for detection of apoptosis. *J Histochem Cytochem*. 2003;51:873-885.
[42] Lovborg H, Gullbo J, Larsson R. Screening for apoptosis--classical and emerging techniques. *Anticancer Drugs*. 2005; 16:593-599.
[43] Kohler C, Orrenius S, Zhivotovsky B. Evaluation of caspase activity in apoptotic cells. *J Immunol Methods*. 2002;256: 97-110.
[44] Darzynkiewicz Z, Huang X, Okafuji M. Detection of DNA strand breaks by flow and laser scanning cytometry in studies of apoptosis and cell proliferation (DNA replication). *Methods Mol Biol*. 2006;314:81-93.
[45] Barrett KL, Willingham JM, Garvin AJ, Willingham MC. Advances in cytochemical methods for detection of apoptosis. *J Histochem Cytochem*. 2001;49:821-832.
[46] Micoud F, Mandrand B, Malcus-Vocanson C. Comparison of several techniques for the detection of apoptotic astrocytes in vitro. *Cell Prolif*. 2001;34:99-113.
[47] Bedner E, Li X, Gorczyca W, Melamed MR, Darzynkiewicz Z. Analysis of apoptosis by laser scanning cytometry. *Cytometry*. 1999;35:181-195.
[48] Soldani C, Scovassi AI, Canosi U, et al. Multicolor fluorescence technique to detect apoptotic cells in advanced coronary atherosclerotic plaques. *Eur J Histochem*. 2005;49:47-52.
[49] Darzynkiewicz Z, Huang X, Okafuji M, King MA. Cytometric methods to detect apoptosis. *Methods Cell Biol*. 2004;75: 307-341.
[50] Darzynkiewicz Z, Bruno S, Del Bino G, et al. Features of apoptotic cells measured by flow cytometry. *Cytometry*. 1992;13:795-808.
[51] Vermes I, Haanen C, Reutelingsperger C. Flow cytometry of apoptotic cell death. *J Immunol Methods*. 2000;243:167-190.
[52] Hunter AL, Choy JC, Granville DJ. Detection of apoptosis in cardiovascular diseases. *Methods Mol Med*. 2005;112:277-289.
[53] Glisic-Milosavljevic S, Waukau J, Jana S, et al. Comparison of apoptosis and mortality measurements in peripheral blood mononuclear cells (PBMCs) using multiple methods. *Cell Prolif*. 2005;38:301-311.
[54] Gorczyca W, Bruno S, Darzynkiewicz RJ, Gong J, Darzynkiewicz Z. DNA strand breaks occurring during apoptosis: Their early in situ detection by the terminal deoxynucleotidyl transferase and nick translation assays and prevention by serine protease inhibitors. *Int J Oncol*. 1992;1:639-648.
[55] Hewitson TD, Bisucci T, Darby IA. Histochemical localization of apoptosis with in situ labeling of fragmented DNA. *Methods Mol Biol*. 2006;326:227-34.
[56] Otsuki Y, Li Z, Shibata MA. Apoptotic detection methods--from morphology to gene. *Prog Histochem Cytochem*. 2003; 38:275-339.
[57] Krutzik PO, Nolan GP. Intracellular phospho-protein staining techniques for flow cytometry: minitoring single cell signaling events. *Cytometry A*. 2003;55:61-70.
[58] Krutzik PO, Clutter MR, Nolan GP. Coordinate analysis of murine immune cell surface markers and intracellular phosphoproteins by flow cytometry. *J Immunol*. 2005;175: 2357-2365.
[59] Deptala A, Bedner E, Gorczyca W, Darzynkiewicz Z. Activation of nuclear factor kappa B (NF-kappaB) assayed by laser scanning cytometry (LSC). *Cytometry*. 1998;33:376-382.
[60] Fanning SL, George TC, Feng D, et al. Receptor Cross-Linking on Human Plasmacytoid Dendritic Cells Leads to the Regulation of IFN-gamma Production. *J Immunol*. 2006;177: 5829-5839.

[61] Kim J, Kim D, Chung J. Replication protein a 32 kDa subunit (RPA p32) binds the SH2 domain of STAT3 and regulates its transcriptional activity. *Cell Biol Int*. 2000;24:467-473.
[62] Yu Z, Zhang W, Kone BC. Signal transducers and activators of transcription 3 (STAT3) inhibits transcription of the inducible nitric oxide synthase gene by interacting with nuclear factor kappaB. *Biochem J*. 2002;367:97-105.
[63] Swick L, Kapatos G. A yeast 2-hybrid analysis of human GTP cyclohydrolase I protein interactions. *J Neurochem*. 2006;97: 1447-1455.
[64] Miyashita T. Confocal microscopy for intracellular co-localization of proteins. Methods Mol Biol, 2004; 261: 399-410
[65] Voss TC, Demarco IA, Day RN. Quantitative imaging of protein interactions in the cell nucleus. Biotechniques, 2005; 38: 413-424
[66] Cherry RJ, Morrison IE, Karakikes I, et al. Measurements of associations of cell-surface receptors by single-particle fluorescence imaging. *Biochem Soc Trans*. 2003;31:1028-1031.
[67] Nohe A, Petersen NO. Analyzing for co-localization of proteins at a cell membrane. *Curr Pharm Biotechnol*. 2004;5: 213-220.
[68] Gillard GO, Farr AG. Features of Medullary Thymic Epithelium Implicate Postnatal Development in Maintaining Epithelial Heterogeneity and Tissue-Restricted Antigen Expression. *J Immunol*. 2006;176:5815-5824.
[69] Hall B, Perry D, Brawley J, et al. Multispectral high content cellular analysis using a flow based imaging cytometer. *Cytometry A*. 2004;59A:152.
[70] Shapiro HM. Practical Flow Cytometry. ed Fourth. John Wiley & Sons, Inc., 2005 [71] Klein AB, Witonsky SG, Ahmed SA, et al. Impact of different cell isolation techniques on lymphocyte viability and function. *J Immunoassay Immunochem*. 2006;27:61-76.
[72] Totino PR, Riccio EK, Corte-Real S, Daniel-Ribeiro CT, de Fatima Ferreira-da-Cruz M. Dexamethasone has pro-apoptotic effects on non-activated fresh peripheral blood mononuclear cells. *Cell Biol Int*. 2006;30:133-137.
[73] Njoh KL, Patterson LH, Zloh M, et al. Spectral analysis of the DNA targeting bisalkylaminoanthraquinone DRAQ5 in intact living cells. *Cytometry A*. 2006;69:.805-814.
[74] Martin RM, Leonhardt H, Cardoso MC. DNA labeling in living cells. *Cytometry A*. 2005;67:45-52.
[75] Yuan CM, Douglas-Nikitin VK, Ahrens KP, et al. DRAQ5-based DNA content analysis of hematolymphoid cell subpopulations discriminated by surface antigens and light scatter properties. *Cytometry B Clin Cytom*. 2004;58:47-52.

Submitted: 28 August, 2007
Accepted after reviews: 5 September, 2007